Fully Distributed Economic Dispatch for Cyber-physical Power System with Time Delays and Channel Noises

Yuhang Zhang, Ming Ni, and Yonghui Sun

***Abstract*—Economic dispatch problem (EDP) is a fundamental optimization problem in power system operation, which aims at minimizing the total generation cost. In fact, the power grid is becoming a cyber-physical power system (CPPS). Therefore, the quality of communication is a key point. In this paper, considering two important factors, i.e., time delays and channel noises, a fully distributed consensus based algorithm is proposed for solving EDP. The critical maximum allowable upper bounds of heterogeneous communication delays and self-delays are obtained. It should be pointed out that the proposed algorithm can be robust against the time-varying delays and channel noises considering generator constraints. In addition, even with time-varying delays and channel noises, the power balance of supply and demand is not broken during the optimization. Several simulation studies are presented to validate the correctness and superiority of the developed results.**

***Index Terms*—Distributed economic dispatch, consensus-based algorithm, cyber-physical power system, time delay, channel noises.**

I. Introduction

ECONOMIC dispatch strategy for power system has always been a research hotspot. In the past twenty years, a great amount of algorithms such as genetic algorithm [1], particle swarm optimization (PSO) algorithm [2], and deep reinforcement learning algorithm [3] have been utilized to solve economic dispatch problem (EDP). However, these traditional algorithms for EDP are centralized algorithms which require a center controller to collect information and send control signals. Due to the unsatisfactory performance of centralized scheduling and control modes such as communication congestion, poor flexibility and scalability, single point failure and some privacy issues, distributed economic dispatch (DED) strategy becomes a popular research topic recently, which is more suitable for cyber-physical power system (CPPS) with increasing distributed energy resources [4]. Various distributed methods have been gradually proposed and applied in the real-time economic dispatch [5]-[11]. Especially, consensus-based algorithms have been used widely for their excellent performance. In [12], a distributed leader-follower algorithm for EDP is presented, while a leader agent is required to store the deviation value between power output and load demand. Without a leader node, a two-level strategy is designed in [13]. In [14], with a feasible initialization, the optimal active power output and margin cost can be obtained by the proposed consensus-based algorithm. In [15], a robust distributed power allocation strategy considering cyber attack is proposed. The other relevant results can be found in [16]-[19].

It is worth noting that all the aforementioned distributed consensus-based algorithms are implemented under the perfect communication network. However, in the modern CPPS, the power grid and the cyber network interact with each other closely [20], [21]. Hence, the communication quality will largely influence the reliability and stability of power systems. In the actual communication network, the information receiving from neighbors is always with time delays induced by the physical distance among them [22]. Therefore, based on the existing distributed consensus-based algorithms, the effects of communication time delays and channel noises are required to be investigated. Meanwhile, it is also necessary to design a novel approach to adapt to the imperfect communication environment. In [23], the effects of delays on the double-level consensus-based algorithm are discussed. According to the case studies presented in [24], it is found that there are some negative results considering time delays, for example, the convergence rate is slower and the results converge to wrong values or even diverge. In [25], a distributed algorithm for EDP on microgrids considering time-varying delays is presented. The distributed continuous-time algorithm proposed in [26] can calculate the optimal economic dispatch result under undirected switching graphs. In [27], the allowable upper bound of time delays is obtained, but only the uniform constant delays are considered and the genera-

Manuscript received: December 3, 2020; revised: March 15, 2021; accepted: July 26, 2021. Date of CrossCheck: July 26, 2021. Date of online publication: September 15, 2021.

This work was supported by the National Natural Science Foundation of China (No. 61833008), the National Natural Science Foundation of China-State Grid Joint Fund for Smart Grid (No. U1966202), and the Six Talent Peaks High Level Project of Jiangsu Province (No. 2017-XNY-004).

Y. Zhang and Y. Sun (corresponding author) are with the College of Energy and Electrical Engineering, Hohai University, Nanjing 210098, China (e-mail: zhangyuhang0826@126.com; sunyonghui168@gmail.com).

M. Ni is with the NARI Group Corporation (State Grid Electric Power Research Institute), Nanjing 211106, China, and he is also with NARI Technology Co., Ltd., Nanjing 211106, China, and State Key Laboratory of Smart Grid Protection and Control, Nanjing 211106, China (e-mail: ni-ming@sgepri.sgcc.com.cn).

DOI: 10.35833/MPCE.2020.000847

tion constraints are ignored. Reference [28] analyzes the effects of the heterogeneous time delays on a consensus-based algorithm and obtain the maximum allowable delay theoretically. However, the above-mentioned algorithms only consider the communication delays, while the self-delays are never considered. In fact, a communication unit always has self-delays caused by delayed data measurements and by pre-treating received information. The self-delays can also degrade the performance or even cause the instability of power systems. Only few studies consider EDP with different self-delays and communication delays simultaneously [29], without consideration of the impacts of channel noise, which is also an important factor.

In our previous work [30], only the homogeneous time delays were investigated. In this paper, the impacts of heterogeneous time delays and channel noises are taken into account. Besides, the cases on time-varying delays, time-varying power demand, and switching topology are also analyzed. The major contributions of this study can be summarized as follows.

1) An effective fully DED strategy is presented for CPPS under non-ideal communication environment. The sum of load demands is calculated in a distributed fashion.

2) The proposed algorithm is suitable for online operation. The global power balance constraint will always be satisfied even with the effect of uncertain delays.

3) The strict allowable range of heterogeneous time delays is derived. Furthermore, the self-delays are also considered in the theoretical results.

4) The effects of time-varying delays and channel noises are investigated considering generator constraints and time-varying power demand. It verifies that the proposed algorithm can be better applied in the actual system under a non-ideal communication environment.

The rest of this paper is organized as follows. (Section II describes the concepts of CPPS, graph theory, EDP, and distributed consensus-based algorithm.) Then, (a fully distributed consensus-based algorithm for solving EDP in the CPPS considering time delays and channel noises is provided in Section III, where the theoretical analysis is also presented.) (Several case studies are given in Section IV to evaluate the effectiveness of the proposed algorithm.) Finally, Section V draws the conclusions.

II. Preliminary

A. Architecture of CPPS

The architecture of CPPS is demonstrated in Fig. 1. Each generator node or load node corresponds to an agent with communication and computing capabilities. Communication links among agents are flexible, which may not be the same as the physical links. In this paper, we mainly investigate the power communication layer in CPPS.

B. Graph Theory

$G=(V,E)$ describes the network topology of the cyber layer in CPPS. $V=\{V_1, V_2, \ldots, V_n\}$ and $E\subseteq V\times V$ denote the communication nodes and the communication links, respectively. The graph G denotes to an undirected graph with no graph loops.

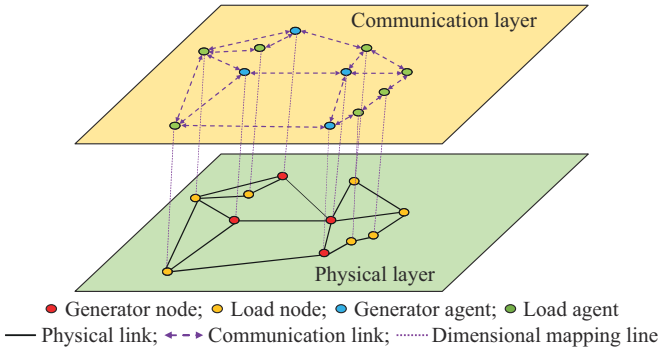

Fig. 1. Architecture of CPPS.

The adjacency matrix $\boldsymbol{A}=(a_{ij})_{n\times n}$ describes the connectivity between communication nodes. The diagonal element $a_{ii}=0$, and $a_{ij}=1$ if nodes i and j are connected, otherwise $a_{ij}=0$. $N_i=\{V_j\in V|(V_j,V_i)\in E\}$ denotes the neighbour nodes of node i. $d_i=\sum_{j\in N_i}a_{ij}$ denotes the degree of node i. The element of the corresponding Laplacian matrix $\boldsymbol{L}$ is given as:

$$\begin{cases} l_{ii}=\sum_{i\neq j}a_{ij} \\ l_{ij}=-a_{ij} \end{cases} \tag{1}$$

C. EDP

The generation cost function is formulated in a quadratic form [16] as:

$$C_i(P_i)=\frac{(P_i-\alpha_i)^2}{2\beta_i}+\gamma_i \tag{2}$$

where $\alpha_i\leq 0$, $\beta_i>0$, and $\gamma_i\leq 0$ are the cost coefficients of generator unit i; and P_i is the active power of generator unit i.

The classical EDP aims at minimizing the total generation cost subject to the power balance constraint and the generator output constraints. Assume there are n generator units, the EDP is formulated by:

$$\min\sum_{i=1}^{n}C_i(P_i) \tag{3}$$

s.t.

$$\sum_{i\in S_G}P_i=\sum_{j\in S_L}P_j=P_{load} \tag{4}$$

$$P_i^{\min}\leq P_i\leq P_i^{\max}\quad i\in S_G \tag{5}$$

where P_j is the local load demand of unit j; P_{load} is the sum of all local demands in a system; S_G is the set of all generators; S_L is the set of all loads; and $P_i^{\min}$ and $P_i^{\max}$ are the lower and upper output power limits, respectively.

D. Distributed Consensus-based Algorithm

The distributed consensus-based algorithm optimizes the global objective by using local and neighbor information. In general, the state updating protocol of agent is briefly represented as:

$$x_i(t+1)=x_i(t)+\sum_{j=1}^{N}a_{ij}(x_j(t)-x_i(t))=x_i(t)+\sum_{j=1}^{N}(-l_{ij}x_j(t)) \tag{6}$$

where $x_i(t)$ and $x_j(t)$ are the states of agents i and j at itera-

tion t, respectively; and N is the number of agents in the communication network.

III. DED for CPPS with Time Delays and Channel Noises

A. CPPS Unit Framework

In CPPS, the security and stability of system operation rely on the coordination and cooperation of each CPPS unit. The structure of a CPPS unit is illustrated in Fig. 2. Communication units can send and receive the information to their neighbor units. N_i^{in} denotes the neighbors which send the information to unit i while N_i^{out} denotes the neighbors which receive the information from unit i. The information processing unit is important to achieve the global control. On one hand, these units monitor and sample the continuous operating states of physical devices. On the other hand, they process the information of neighbors, calculate the outgoing information, and make the control instructions. In the following, DED is based on this framework.

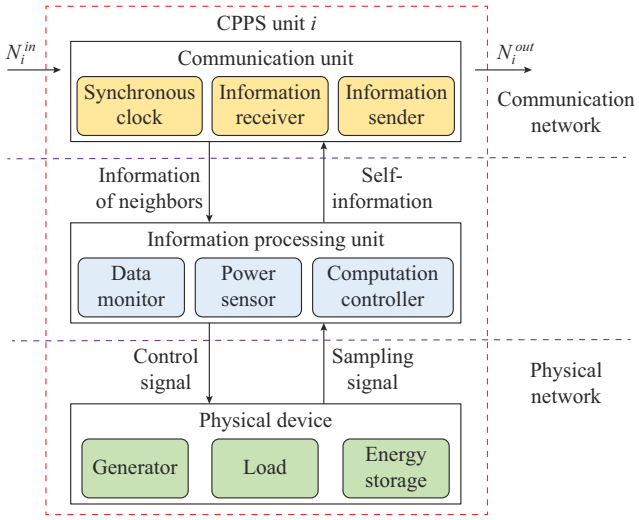

Fig. 2. Structure of a CPPS unit.

B. Total Power Demand Discovery Algorithm

In power systems, the power demand of each load unit is time-varying in practical, hence, the total power demand P_{load} is time-varying as well. Note that most existing results use the centralized methods containing central controllers to figure out P_{load}. How to obtain P_{load} in a distributed way for each agent is an interesting issue to be addressed. Herein, a fast distributed finite-step algorithm is designed to find P_{load}.

In most DED strategy, the communication topology connected by generator agents is adopted. Herein, load agents should also be considered in the cyber network. The new bigger communication topology is $\tilde{G}$ and its Laplacian matrix is $\tilde{\boldsymbol{L}}$. $D_i(k)$ is defined as the communication state of agent i at step k, $i \in S_G \bigcup S_L$, and $|S_G| = n$, $|S_L| = m$. The K-step algorithm [31], [32] is applied to calculate P_{load} for each agent. The algorithm is given as follows, where $w_{ij}(k)$ is the weight coefficient of the link at iteration k.

Algorithm 1: discovery algorithm of total power demand

Step 1: initialize the communication state $D_i(0)$:

$$D_i(0) = \begin{cases} 0 & i \in S_G, i = 1, 2, \ldots, n \\ P_i & i \in S_L, i = n+1, n+2, \ldots, n+m \end{cases}$$

Step 2: compute K different nonzero eigenvalues of $\tilde{\boldsymbol{L}}$, i.e., $\mu_2, \mu_3, \ldots, \mu_{K+1}$

Step 3: **if** $k < K$, update communication weight:

$$w_{ij}(k) = \begin{cases} 1 - \dfrac{d_i}{\mu_{k+1}} & j = i \\ \dfrac{1}{\mu_{k+1}} & j \in N_i \\ 0 & \text{otherwise} \end{cases}$$

Then, compute the state value for each agent:

$$D_i(k+1) = w_{ii}(k) D_i(k) + \sum_{j \in N_i} w_{ij}(k) D_j(k) \quad i = 1, 2, \ldots, n+m$$

Step 4: **else if** $k = K$, figure out P_{load}:

$$P_{load} = (n+m) D_i(K) \quad i = 1, 2, \ldots, n+m$$

end if

Step 5: **end if**

Remark 1 The initialization process is at *Step 1* and *Step 2*. At *Step 3*, both $w_{ij}(k)$ and $D_i(k+1)$ are updated at each iteration. The total number of iteration steps is K, which is determined by $\tilde{\boldsymbol{L}}$. There is no need to preload the Laplacian matrix. When the communication topology changes, each agent can update the Laplacian matrix by itself automatically using a novel graph discovery algorithm [31]. At *Step 4*, we obtain $D_1(K) = D_2(K) = \ldots = D_{n+m}(K) = \dfrac{1}{n+m} \sum_{i=1}^{n+m} D_i(0)$. Using Algorithm 1, each agent obtains P_{load} in finite steps in a distributed manner.

C. DED with Heterogeneous Time Delays

In classic DED algorithm, the incremental cost for agent i is:

$$\lambda_i = \frac{\partial C_i(P_i)}{\partial P_i} = \frac{P_i - \alpha_i}{\beta_i} \quad i = 1, 2, \ldots, n \tag{7}$$

The incremental cost is utilized as the consensus variable. The distributed algorithm under the ideal communication environment is designed as:

$$\begin{cases} \lambda_i(t+1) = \dfrac{P_i(t) - \alpha_i}{\beta_i} + \varepsilon \sum_{j=1}^{n} (-l_{ij} \beta_i^{-1} \lambda_j(t)) \\ P_i(t+1) = P_i(t) + \rho \sum_{j=1}^{n} (-l_{ij} \lambda_j(t)) \end{cases} \tag{8}$$

where ε and ρ are the positive gains for adjusting the convergence speed. The larger ε and ρ are, the faster the convergence speed of the distributed iteration process is. The feasible positive gains are bounded by $0 < \rho \le 4/a_{\max}$ and $0 < \varepsilon \le 3/a_{\max}$, where $a_{\max}$ is the maximum eigenvalue of $\boldsymbol{\beta}^{-\frac{1}{2}} \boldsymbol{L} \boldsymbol{\beta}^{-\frac{1}{2}}$, $\boldsymbol{\beta} = \text{diag}\{\beta_1, \beta_2, \ldots, \beta_n\}$ [36].

There are two-layer protocols in algorithm (8). Firstly, the incremental cost information is updated by local power information and neighbor incremental cost information. Then, the power information is updated by the local power information of previous iteration as well as the neighbor incremental cost information. To ensure the privacy, only the incremental cost

information is needed to exchange, which is different from the algorithm in [8], [16].

Remark 2 According to the definition of Laplacian matrix, it is easy to get $\mathbf{1}^{\mathrm{T}}\boldsymbol{L}=\mathbf{0}$. Thus, $\sum_{i=1}^{n}P_i(t+1)=\sum_{i=1}^{n}P_i(t)$. So the total output power is invariant at each iteration and only determined by the initialization.

Since we have analyzed the case of homogeneous time delays in our previous work, the heterogeneous communication time delays τ_{ij} and self-delays T_{ij} are considered in this case. Self-delays are caused by delayed relative measurements and computation in the information processing unit shown in Fig. 2. Considering the two types of delays, the distributed algorithm is described as:

$$\sum_{i=1}^{n}P_i(0)=P_{load}=(n+m)D_i(K) \tag{9}$$

$$\lambda_i(t+1)=\frac{P_i(t)-\alpha_i}{\beta_i}+\frac{\rho}{\beta_i}\sum_{j\in N_i}a_{ij}[\lambda_j(t-\tau_{ij})-\lambda_i(t-T_{ij})] \tag{10}$$

$$P_i(t+1)=P_i(t)+\rho\sum_{j\in N_i}a_{ij}[\lambda_j(t-\tau_{ij})-\lambda_i(t-T_{ij})] \tag{11}$$

Herein, the upper bound of the maximum allowable delay is denoted by $\bar{\tau}$, i.e., $\tau_{ij}\le\bar{\tau}$ and $T_{ij}\le\bar{\tau}$. In order to describe the topology graph with time delays, we further modify the adjacency matrix, degree matrix with communication delays, and degree matrix with self-delays as $\boldsymbol{A}_\tau(s)=\left(a_{ij}\mathrm{e}^{-\tau_{ij}s}/d_i\right)$, $\boldsymbol{D}_\tau(s)=\mathrm{diag}\left\{\frac{1}{d_i}\sum_{j=1}^{n}a_{ij}\mathrm{e}^{-\tau_{ij}s}\right\}$, $\boldsymbol{D}_T(s)=\mathrm{diag}\left\{\frac{1}{d_i}\sum_{j=1}^{n}a_{ij}\mathrm{e}^{-T_{ij}s}\right\}$, respectively.

Based on the algorithms (9)-(11), the allowable range of heterogeneous time delays can be derived by Theorem 1.

Theorem 1 Under the algorithm (9)-(11), λ_i can converge to the optimal value if $\bar{\tau}$ satisfies:

$$\bar{\tau}<\min\left(\frac{1}{2\rho\beta_i^{-1}d_i}\right)\quad i=1,2,\ldots,n \tag{12}$$

Proof Combining (10) and (11), we can obtain:

$$\lambda_i(t+1)=\lambda_i(t)+\rho\beta_i^{-1}\sum_{j=1}^{n}a_{ij}[\lambda_j(t-\tau_{ij})-\lambda_i(t-T_{ij})] \tag{14}$$

Similarly, taking the Laplace transform for (14) yields:

$$s\lambda_i(s)-\lambda_i(0)=\rho\beta_i^{-1}\left(\sum_{j=1}^{n}a_{ij}\mathrm{e}^{-\tau_{ij}s}\lambda_j(s)-\sum_{j=1}^{n}a_{ij}\mathrm{e}^{-T_{ij}s}\lambda_i(s)\right) \tag{15}$$

Let $\boldsymbol{\lambda}(s)=[\lambda_1(s),\lambda_2(s),\ldots,\lambda_n(s)]^{\mathrm{T}}$, we can obtain:

$$s\boldsymbol{\lambda}(s)-\boldsymbol{\lambda}(0)=\rho\boldsymbol{\beta}^{-1}(\boldsymbol{A}_\tau(s)-\boldsymbol{D}_T(s))\boldsymbol{\lambda}(s) \tag{16}$$

Then, we can obtain:

$$\boldsymbol{\lambda}(s)=[s\boldsymbol{I}+\mathrm{diag}\{\rho\beta_i^{-1}d_i\}(\boldsymbol{D}_T(s)-\boldsymbol{A}_\tau(s))]^{-1}\boldsymbol{\lambda}(0) \tag{17}$$

Hence, the characteristic equation can be obtained as:

$$\det\{s\boldsymbol{I}+\mathrm{diag}\{\rho\beta_i^{-1}d_i\}(\boldsymbol{D}_T(s)-\boldsymbol{A}_\tau(s))\}=0 \tag{18}$$

Let $\boldsymbol{G}_r(s)=-\mathrm{diag}\{\rho\beta_i^{-1}d_i/(s+2\rho\beta_i^{-1}d_i)\}[2\boldsymbol{I}-(\boldsymbol{D}_T(s)-\boldsymbol{A}_\tau(s))]$. According to (19), we can prove that $\det\{s\boldsymbol{I}+\mathrm{diag}\{\rho\beta_i^{-1}d_i\}\cdot(\boldsymbol{D}_T(s)-\boldsymbol{A}_\tau(s))\}=0$ and $\det\{\boldsymbol{I}+\boldsymbol{G}_r(s)\}=0$ have the same roots in the open right-half complex plane.

$$\begin{aligned}\boldsymbol{I}+\boldsymbol{G}_r(s)&=\boldsymbol{I}-\mathrm{diag}\left\{\frac{\rho\beta_i^{-1}d_i}{s+2\rho\beta_i^{-1}d_i}\right\}[2\boldsymbol{I}-(\boldsymbol{D}_T(s)-\boldsymbol{A}_\tau(s))]=\\&\mathrm{diag}\left\{\frac{\rho\beta_i^{-1}d_i}{s+2\rho\beta_i^{-1}d_i}\right\}(\boldsymbol{D}_T(s)-\boldsymbol{A}_\tau(s))+\mathrm{diag}\left\{\frac{s}{s+2\rho\beta_i^{-1}d_i}\right\}\boldsymbol{I}=\\&\mathrm{diag}\left\{\frac{1}{s+2\rho\beta_i^{-1}d_i}\right\}[s\boldsymbol{I}+\mathrm{diag}\{\rho\beta_i^{-1}d_i\}(\boldsymbol{D}_T(s)-\boldsymbol{A}_\tau(s))]\end{aligned} \tag{19}$$

According to [29], the spectrum of $\boldsymbol{G}_r(s)$ satisfies:

$$\sigma(\boldsymbol{G}_r(\mathrm{j}\omega))\subseteq-Co\left\{\frac{\rho\beta_i^{-1}d_i}{\mathrm{j}\omega+2\rho\beta_i^{-1}d_i}\Omega(\mathrm{j}\omega\bar{\tau}):i=1,2,\ldots,n\right\} \tag{20}$$

$$\Omega(\mathrm{j}\omega\bar{\tau})=Co\{2-\mathrm{e}^{-\mathrm{j}\psi}+\mathrm{e}^{-\mathrm{j}\varphi},2-\mathrm{e}^{\mathrm{j}\psi}-\mathrm{e}^{-\mathrm{j}\varphi}:\psi,\varphi\in[0,\omega\bar{\tau}]\} \tag{21}$$

where $Co\{\cdot\}$ denotes the convex hull; and ω is the angular frequency.

Then, the roots of $\det\{\boldsymbol{I}+\boldsymbol{G}_r(s)\}=0$ are not in the open right-half complex plane if

$$-1\notin-Co\left\{\frac{\rho\beta_i^{-1}d_i}{\mathrm{j}\omega+2\rho\beta_i^{-1}d_i}\Omega(\mathrm{j}\omega\bar{\tau}):i=1,2,\ldots,n\right\} \tag{22}$$

i.e.,

$$Co\left\{\left(2+\frac{\mathrm{j}\omega}{\rho\beta_i^{-1}d_i}\right)^{-1}:i=1,2,\ldots,n\right\}^{-1}\cap\Omega(\mathrm{j}\omega\bar{\tau})=\varnothing \tag{23}$$

It is easy to obtain:

$$\begin{cases}\mathrm{Re}\left(2+\dfrac{\mathrm{j}\omega}{\rho\beta_i^{-1}d_i}\right)=2\\[2ex]\mathrm{Im}\left(2+\dfrac{\mathrm{j}\omega}{\rho\beta_i^{-1}d_i}\right)=\dfrac{\omega}{\rho\beta_i^{-1}d_i}\end{cases} \tag{24}$$

Thus, the convex hull of the above formula is a line. Then, we consider the convex hull of $\Omega(\mathrm{j}\omega\bar{\tau})$, which contains two cases.

1) Case 1: $\omega\bar{\tau}<\pi/2$.

For convenience, the convex hull of $\Omega(\mathrm{j}\omega\bar{\tau})$ in this case and the locus of $2+\mathrm{j}\omega/(\rho\beta_i^{-1}d_i)$ are illustrated in Fig. 3. In order to ensure that the intersection is an empty set, the imaginary part of $2+\mathrm{j}\omega/(\rho\beta_i^{-1}d_i)$ must satisfy:

$$\frac{\omega}{\rho\beta_i^{-1}d_i}>2\tan\left(\frac{\omega\bar{\tau}}{2}\right) \tag{25}$$

Together with $\omega\bar{\tau}<\pi/2$, we can obtain:

$$\rho\beta_i^{-1}d_i\bar{\tau}<\frac{1}{2} \tag{26}$$

Furthermore, we can obtain:

$$\bar{\tau}<\min\left\{\frac{1}{2\rho\beta_i^{-1}d_i}\right\}\quad i=1,2,\ldots,n \tag{27}$$

2) Case 2: $\pi/2<\omega\bar{\tau}<2\pi$.

Similarly, the convex hull of $\Omega(\mathrm{j}\omega\bar{\tau})$ in this case and the locus of $2+\mathrm{j}\omega/(\rho\beta_i^{-1}d_i)$ are obtained as shown in Fig. 4. Obviously, the intersection is not empty if the imaginary part of $2+\mathrm{j}\omega/(\rho\beta_i^{-1}d_i)$ is less than 2. Thus, we can obtain:

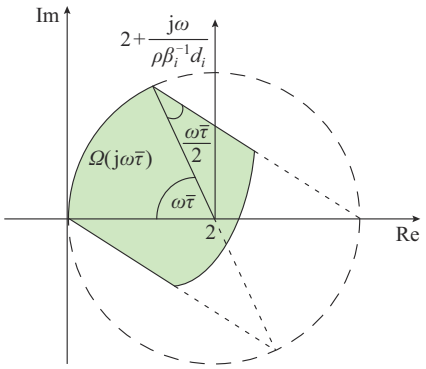

Fig. 3. Convex hull of $\Omega(j\omega\bar{\tau})$ in case 1 and locus of $2+j\omega/(\rho\beta_i^{-1}d_i)$.

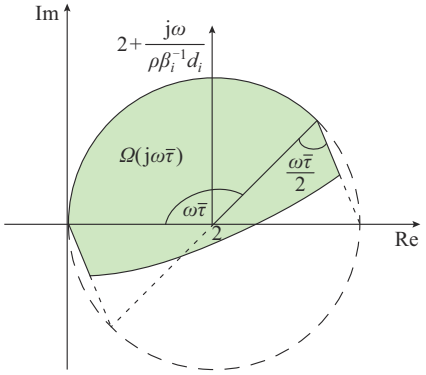

Fig. 4. Convex hull of $\Omega(j\omega\bar{\tau})$ in case 2 and locus of $2+j\omega/(\rho\beta_i^{-1}d_i)$.

$$\frac{\omega}{\rho\beta_i^{-1}d_i}<2 \tag{28}$$

Based on $\omega\bar{\tau}>\pi/2$, we can obtain:

$$\frac{\rho\beta_i^{-1}d_i}{\omega}\omega\bar{\tau}>\frac{1}{2}\frac{\pi}{2}=\frac{\pi}{4} \tag{29}$$

Furthermore, we can obtain:

$$\bar{\tau}>\frac{\pi}{4\rho\beta_i^{-1}d_i} \tag{30}$$

Thus, it is concluded that the intersection is empty if $\bar{\tau}$ satisfies:

$$\bar{\tau}<\min\left\{\frac{\pi}{4\rho\beta_i^{-1}d_i}\right\}\quad i=1,2,\ldots,n \tag{31}$$

According to the analysis of the above two cases, we can finally obtain:

$$\bar{\tau}<\min\left\{\frac{\pi}{4\rho\beta_i^{-1}d_i},\frac{1}{2\rho\beta_i^{-1}d_i}\right\}=\min\left\{\frac{1}{2\rho\beta_i^{-1}d_i}\right\}\quad i=1,2,\ldots,n \tag{32}$$

Remark 3 Theorem 1 shows that the delay tolerance of algorithm (9)-(11) is determined by the gain coefficient ρ, the cost coefficient β_i, and the degree d_i. The bigger the degree d_i is and the stronger-connected the communication topology is, the faster convergence rate is. However, the delay upper bound is smaller, which leads to the poorer robustness against time delays. Therefore, there is a tradeoff between the convergence speed and delay tolerance. In a practical system, since the network topology is usually determined, the gain ρ is designed to adjust the convergence speed and delay tolerance ability according to the actual demand. Besides, we also consider the impact of self-delays, which is more completed compared with the existing results [27], [28].

D. DED with Time-varying Delays and Channel Noises

Besides time-varying delays and channel noises, the generation output constraints are considered. In algorithms (9)-(11), the gain coefficient ρ is a constant, the results are not convergent due to the impacts of the channel noises. Therefore, we transform the gain coefficient into a time-varying form $\rho(t)$, which satisfies:

$$\begin{cases}\sum_{t=0}^{\infty}\rho(t)=+\infty\\ \sum_{t=0}^{\infty}\rho^2(t)<+\infty\end{cases} \tag{33}$$

Then, the improved distributed algorithm considering time-varying delays and channel noises can be obtained as:

$$\begin{cases}\sum_{i=1}^{n}P_i(0)=P_{load}=(n+m)D_i(K)\\ \lambda_i(t+1)=\frac{P_i(t)-\alpha_i}{\varphi_i(t)}+\frac{\rho(t)}{\varphi_i(t)}\sum_{j=1}^{n}[-l_{ij}(t)(\lambda_j(t-\tau(t))+\eta_{ij}(t))]\\ P_i(t+1)=P_i(t)+\rho(t)\sum_{j=1}^{n}[-l_{ij}(t)(\lambda_j(t-\tau(t))+\eta_{ij}(t))]\end{cases} \tag{34}$$

where $\eta_{ij}(t)$ is the channel noise in the communication link from unit i to unit j at instant t; and $\rho(t)=\theta_1\ln(\theta_2 t+1)/(\theta_2 t+1)$, in which $\theta_1>0$ and $\theta_2>0$ are the convergence factors. The expression of $\varphi_i(t)$ is omitted here and can be found in [33].

Considering that the total load demand is time-varying, we have to update P_{load} at time intervals, which are assumed as 15 min [34], [35]. The fully DED with time-varying delays and channel noises is presented by Algorithm 2.

Algorithm 2: fully DED with time-varying delays and channel noises

Step 1: calculate P_{load} by Algorithm 1, i.e., $\sum_{i=1}^{n}P_i(0)=P_{load}=(n+m)D_i(K)$, and set the initial output power $P_i(0)$ of each generator according to its capacity and operation state

Step 2: calculate the optimal incremental cost λ^* and the corresponding output power P_i^* by iterations:

$$\lambda_i(t+1)=\frac{P_i(t)-\alpha_i}{\varphi_i(t)}+\frac{\rho(t)}{\varphi_i(t)}\sum_{j=1}^{n}[-l_{ij}(t)(\lambda_j(t-\tau(t))+\eta_{ij}(t))]$$

$$P_i(t+1)=P_i(t)+\rho(t)\sum_{j=1}^{n}[-l_{ij}(t)(\lambda_j(t-\tau(t))+\eta_{ij}(t))]$$

Step 3: every other 15 min, update the new total power demand P'_{load} by Algorithm 1

Step 4: **if** $\Delta P=P'_{load}-P_{load}\neq 0$, allocate the mismatch power ΔP by the virtual command node
Then, go to *Step 2*
else if $\Delta P=0$, go to *Step 3*
end if

Step 5: **end if**

Remark 4 This algorithm is a fully DED implementation. All the state data are calculated by information exchange among their neighbors. Firstly, P_{load} is figured out us-

ing Algorithm 1 under the communication graph $\tilde{G}$ which contains generator units and load units. Then, the optimal dispatch results are calculated under the communication graph G which contains generator units only. That is to say, load units merely participate in network communication when updating the P_{load}. Thus, the communication burden is alleviated effectively by this algorithm. The result is recalculated every 15 min, so it means the cyber network just needs to switch every 15 min. The switch frequency is acceptable in the future CPPS. Besides, Algorithm 2 is robust to channel noises, which are ignored in the existing results [27], [28].

IV. Case Studies

The case studies are simulated in the MATLAB R2018a environment on a laptop with Intel Core i5-7300U CPU @ 2.60 GHz and 8 GB RAM. The IEEE 14-bus system containing 5 generator units and 9 load units is utilized. The communication topology of the 14-bus CPPS is presented in Fig. 5.

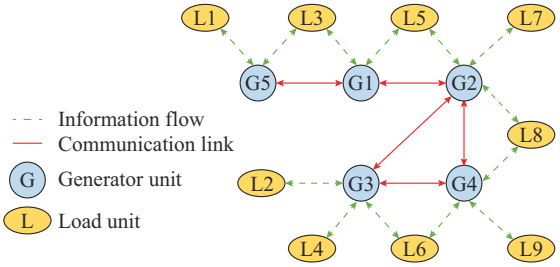

Fig. 5. Communication topology of 14-bus CPPS.

G contains five schedulable generator units only, while $\tilde{G}$ includes all units. For graph G, the sets of neighbours of each unit are denoted as $N_{G1}=\{G2, G5\}$, $N_{G2}=\{G1, G3, G4\}$, $N_{G3}=\{G2, G4\}$, $N_{G4}=\{G2, G3\}$, $N_{G5}=\{G1\}$ and the adjacency matrix $\boldsymbol{A}$ and the Laplacian matrix $\boldsymbol{L}$ are given as:

$$\boldsymbol{A}=\begin{bmatrix}0&1&0&0&1\\1&0&1&1&0\\0&1&0&1&0\\0&1&1&0&0\\1&0&0&0&0\end{bmatrix} \tag{35}$$

$$\boldsymbol{L}=\begin{bmatrix}2&-1&0&0&-1\\-1&3&-1&-1&0\\0&-1&2&-1&0\\0&-1&-1&2&0\\-1&0&0&0&1\end{bmatrix} \tag{36}$$

In the testing power grid, the corresponding parameters of cost functions and capacity constraints of each generator are provided in Table I [33].

A. Total Power Demand Calculation

The power demand of each load is shown in Table II. By using Algorithm 1, we can obtain the average power demand in 13 steps. The iteration process is shown in Fig. 6. The final average value is 107.1429 MW.

TABLE I
Parameters of Cost Functions and Capacity Constraints of Each Generator

Generator	α_i (MW)	β_i (MW^{2}h/\$)	γ_i (\$/h)	$P_i^{\min}$ (MW)	$P_i^{\max}$ (MW)
G1	−2535.2	352.1	−8616.8	150	500
G2	−2535.2	352.1	−8616.8	150	500
G3	−2023.2	257.7	−7631.0	100	400
G4	−826.8	103.7	−3216.7	50	200
G5	−2023.2	257.7	−7631.0	100	400

TABLE II
Power Demand of Each Load

Load	Demand (MW)	Load	Demand (MW)
L1	100	L6	80
L2	240	L7	330
L3	60	L8	50
L4	120	L9	120
L5	400		

Consequently, the total power demand $P_{load}=14\times 107.1429=1500$ MW. Assume that the initial output power of each generator is set as $P_1(0)=400$ MW, $P_2(0)=300$ MW, $P_3(0)=300$ MW, $P_4(0)=150$ MW, $P_5(0)=350$ MW. For convenience, the initial values are used in all the following case studies.

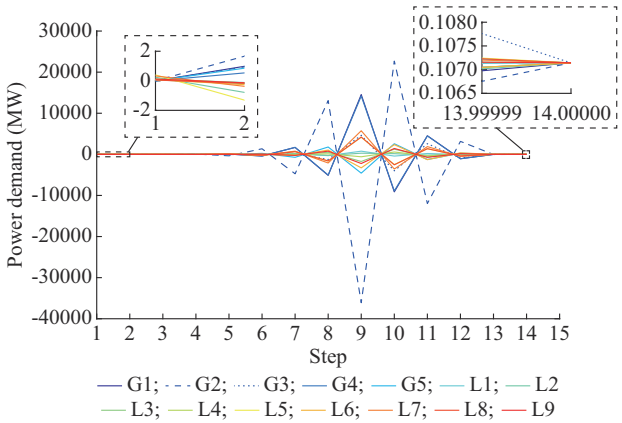

Fig. 6. Power demand calculation results using Algorithm 1.

B. Case Study 1

The heterogeneous time delays including self-delays are considered. Let $\rho=5$, we obtain the allowable delay upper bound $\bar{\tau}=5.1850$ s by Theorem 2. The elements in the communication delay matrix $\boldsymbol{\tau}$ and self-delay matrix $\boldsymbol{T}$ are determined randomly within the allowable range, as shown in (37) and (38), respectively.

$$\boldsymbol{\tau}=\begin{bmatrix}0&5&0&0&4\\4&0&3&5&0\\0&2&0&5&0\\0&3&5&0&0\\4&0&0&0&0\end{bmatrix} \tag{37}$$

$$\boldsymbol{T}=\begin{bmatrix}0&4&0&0&4\\5&0&2&3&0\\0&3&0&5&0\\0&5&5&0&0\\4&0&0&0&0\end{bmatrix} \tag{38}$$

As shown in Fig. 7(a) and (b), under the graph G, the optimal output power results of each generator are obtained as $P_1^{opt}=509.7$ MW, $P_2^{opt}=509.7$ MW, $P_3^{opt}=205.3$ MW, $P_4^{opt}=70.0$ MW, $P_5^{opt}=205.3$ MW, respectively. Meanwhile, the incremental costs converge at about 200 s and the optimal incremental cost $\lambda^{opt}=8.6478$. Then, the graph G is changed into a more strongly connected topology graph G', which is illustrated in Fig. 8. By Theorem 1, the allowable delay upper bound is reduced to $\bar{\tau}'=2.5925$ s. As shown in Fig. 7(c) and (d), under the graph G', the incremental cost does not achieve consensus so that the output power cannot converge. The algebraic connectivities of the graph G and the graph G' are $\lambda_2(G)=0.5188$ and $\lambda_2(G')=5$, respectively. Since the graph G' is more stronger-connected, the system may have a better convergence rate. However, the delay tolerance decreases. Therefore, there exists a trade-off mentioned in Section III.

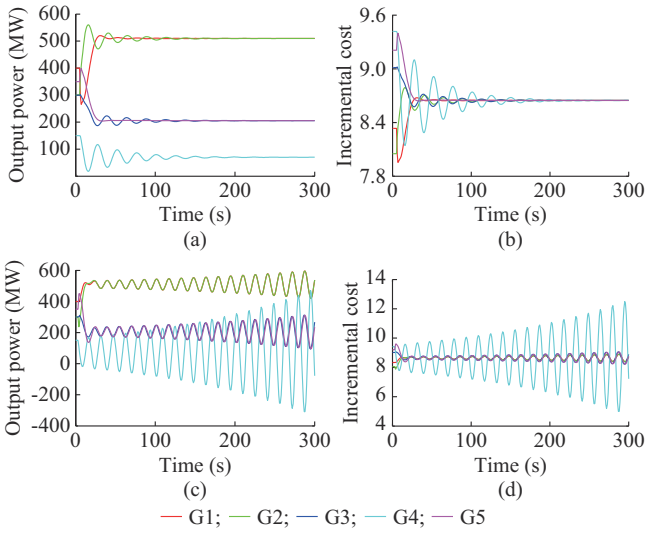

Fig. 7. Simulation results under topology graphs G and G'. (a) Output power under graph G. (b) Incremental costs under graph G. (c) Output power under graph G'. (d) Incremental costs under graph G'.

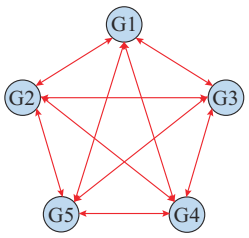

Fig. 8. Strongly connected topology graph G'.

C. Case Study 2

In this case study, the generator constraints, the time-varying power demand, and the time-varying delays are considered. These delays are all assumed to be bounded by $\tau=6$. The tested probability distribution of these delays is given in Table III.

TABLE III
PROBABILITY DISTRIBUTIONS OF TIME DELAYS

Delay	Probability distribution	
	Scenario 1	Scenario 2
0	0.05	0.05
1	0.35	0.05
2	0.35	0.15
3	0.10	0.15
4	0.05	0.30
5	0.05	0.25
6	0.05	0.05

The noises are assumed randomly within the range $[-0.2, 0.2]$, and in this case $\rho(t)=10\ln(0.1t+1)/(0.1t+1)$. The total power demand is 1500 MW at first, then G1 and G2 increase the local demand 50 MW, respectively. The total power demand is updated to 1600 MW at 900 s. Similarly, the total power demand is updated to 1700 MW at 1800 s and 1400 MW at 2700 s, respectively. From Fig. 9, it can be observed that the proposed algorithm can keep fast convergence during the four processes.

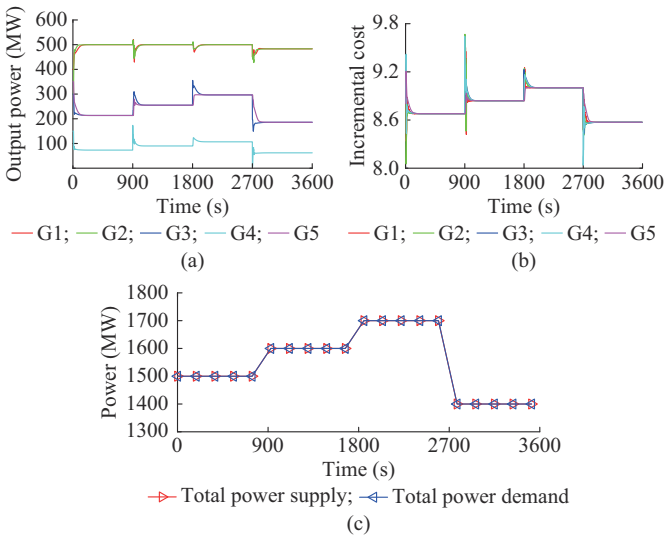

Fig. 9. Simulation results with generation constraints considering time-varying delays of scenario 1 and channel noises. (a) Output power. (b) Incremental costs. (c) Total power supply and demand.

During the first 15 min (process 1), the optimal output power results of each generator are $P_1^{opt}=500.0$ MW, $P_2^{opt}=500.0$ MW, $P_3^{opt}=213.4$ MW, $P_4^{opt}=73.2$ MW, $P_5^{opt}=213.4$ MW. The optimal incremental cost $\lambda^{opt}=8.68$. During the second 15 min (process 2), the optimal output power results of each generator are $P_1^{opt}=500.0$ MW, $P_2^{opt}=500.0$ MW, $P_3^{opt}=255.0$ MW, $P_4^{opt}=90.0$ MW, $P_5^{opt}=255.0$ MW, and $\lambda^{opt}=8.84$. During the third 15 min (process 3), the optimal output power results of each generator are $P_1^{opt}=500.0$ MW, $P_2^{opt}=500.0$ MW, $P_3^{opt}=296.6$ MW, $P_4^{opt}=106.7$ MW, $P_5^{opt}=296.6$ MW, and $\lambda^{opt}=9.00$. During the fourth 15 min (process 4), the op-

timal output power results of each generator are $P_1^{opt}=483.1$ MW, $P_2^{opt}=483.1$ MW, $P_3^{opt}=185.9$ MW, $P_4^{opt}=62.1$ MW, $P_5^{opt}=185.9$ MW, and $\lambda^{opt}=8.57$.

In scenario 2, the probabilities of $\tau=4$ and $\tau=5$ are set to be higher, which affect the stability of the system more seriously. Figure 10 shows that the optimal results are the same as those in scenario 1. Therefore, if the time-varying delays are within the allowable range, Algorithm 2 can maintain good convergence. It verifies that Algorithm 2 has a good robustness to the time delays and it can adapt to the non-ideal communication environment. In addition, the total power demand always equals to the total output power, while the algorithm proposed in [28] cannot ensure the real-time power balance.

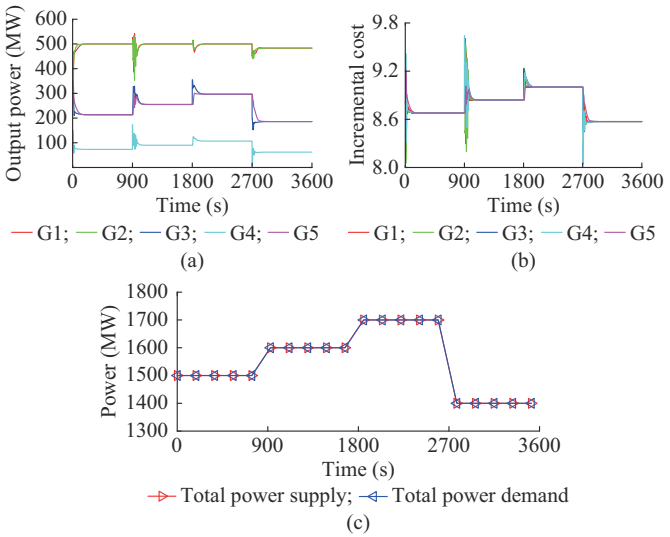

Fig. 10. Simulation results with generation constraints considering time-varying delays of scenario 2 and channel noises. (a) Output power. (b) Incremental costs. (c) Total power supply and demand.

D. Case Study 3

We further test the effectiveness of the proposed algorithm under a more fragile communication condition, i. e., the switching topology. The time delay values are adopted from Table III. During the first 200 s, the disconnected topology A shown in Fig. 11 is used for communication.

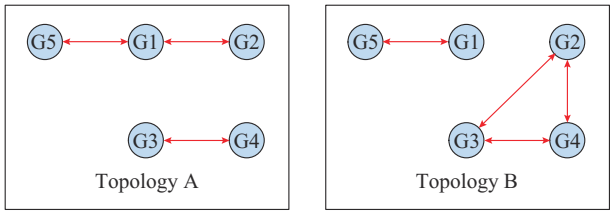

Fig. 11. Switching topology graph.

Then, the topology switches between topology A and topology B every 10 s. The simulation results with switching topology and time-varying delays are shown in Fig. 12. During the first 200 s, the communication topologies are two separate parts so that the results converge to different optimal values. After 200 s, under the switching topology, there exists slight fluctuation during the convergence process because of the effects of time delays. Nevertheless, the whole system finally converges. In addition, no matter under what kind of communication topology, the supply-demand balance of the whole system is not broken. Hence, the proposed algorithm has a good robustness against time delays and adapts to the switching topology.

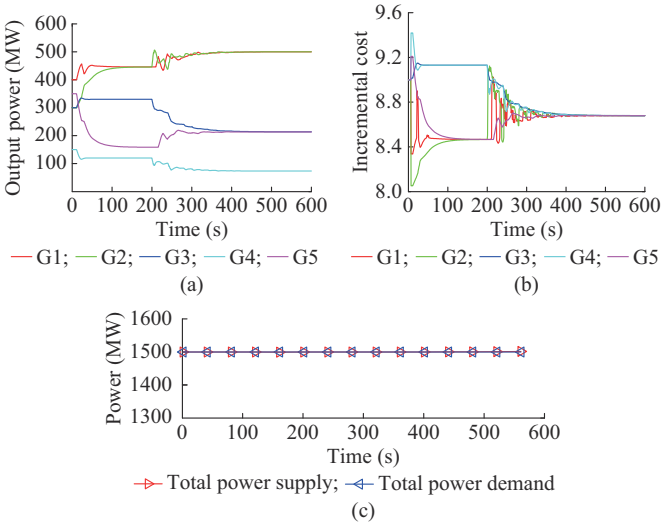

Fig. 12. Simulation results with switching topology and time-varying delays. (a) Output power. (b) Incremental costs. (c) Total power supply and demand.

E. Case Study 4

We further apply the proposed algorithm to a larger system, i. e., IEEE 118-bus system, which is composed by 54 dispatchable generators. Without loss of generality, the cost coefficients of all generators are chosen by the following ranges [33]:

$$\begin{cases} \alpha_i \in [-65, -25] & i=1,2,\ldots,54 \\ \beta_i \in [12, 16] & i=1,2,\ldots,54 \end{cases} \tag{34}$$

The circle topology is used in this case study and several additional edges are added to increase the convergence rate appropriately. According to the determined communication topology, the feasible gain coefficient is calculated as $0<\rho<3.58$. In this case, $\rho(t)=0.3\ln(0.1t+1)/(0.1t+1)$. The time-varying delays and channel noises are bounded like case study 3. The initial output power of each generator is set to be 50 MW. The total load demand is 2700 MW. From Fig. 13, it is verified that the proposed algorithm has a good robustness to the time delays and can well adapt to the non-ideal communication environment in a large system.

V. Conclusion

Considering the non-ideal communication environment, a fully DED algorithm is proposed for CPPS. The heterogeneous communication delays and self-delays are investigated. The allowable delay upper bound can be figured out under a specified communication topology. Furthermore, the algorithm performance under the time-varying delays and channel noises are discussed simultaneously considering the generator constraints, time-varying power demand, and switching topology by several case studies.

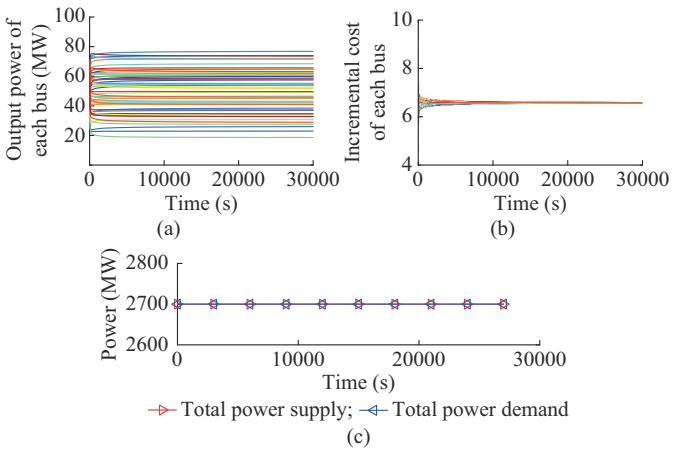

Fig. 13. Simulation results with time-varying delays and channel noises in IEEE 118-bus system. (a) Output power. (b) Incremental costs. (c) Total power supply and demand.

In a practical system, if delays and channel noises have been approximately estimated in advance, based on the theoretical results of Theorem 1, we can appropriately adjust the gain coefficient and the communication topology to satisfy the need for convergence speed and delay tolerance. Therefore, our work is valuable for engineering practice. In our future work, the cyber attack in CPPS will be investigated. And we will further focus on the CPPS modeling and the application of distributed techniques.

REFERENCES

[1] I. G. Damousis, A. G. Bakirtzis, and P. S. Dokopoulos, "Network-constrained economic dispatch using real-coded genetic algorithm," *IEEE Transactions on Power Systems*, vol. 18, no. 1, pp. 198-205, Feb. 2003.

[2] A. I. Selvakumar and K. Thanushkodi, "A new particle swarm optimization solution to nonconvex economic dispatch problems," *IEEE Transactions on Power Systems*, vol. 22, no. 1, pp. 42-51, Feb. 2007.

[3] L. Lin, X. Guan, Y. Peng *et al*., "Deep reinforcement learning for economic dispatch of virtual power plant in internet of energy," *IEEE Internet of Things Journal*, vol. 7, no. 7, pp. 6288-6301, Jul. 2020.

[4] Z. Cheng, J. Duan, and M. Chow, "To centralize or to distribute: that is the question: a comparison of advanced microgrid management systems," *IEEE Industrial Electronics Magazine*, vol. 12, no. 1, pp. 6-24, Mar. 2018.

[5] Z. Cheng and M. -Y. Cheng, "Collaborative distributed AC optimal power flow: a dual decomposition based algorithm," *Journal of Modern Power Systems and Clean Energy*, vol. 9, no. 6, pp. 1414-1423, Nov. 2021.

[6] D. Feng, F. Wu, Y. Zhou *et al*., "Multi-agent-based rolling optimization method for restoration scheduling of distribution systems with distributed generation," *Journal of Modern Power Systems and Clean Energy*, vol. 8, no. 4, pp. 737-749, Jul. 2020.

[7] C. Li, X. Yu, W. Yu *et al*., "Distributed event-triggered scheme for economic dispatch in smart grids," *IEEE Transactions on Industrial Informatics*, vol. 12, no. 5, pp. 1775-1785, Oct. 2016.

[8] Y. Xu and Z. Li, "Distributed optimal resource management based on the consensus algorithm in a microgrid," *IEEE Transactions on Industrial Electronics*, vol. 62, no. 4, pp. 2584-2592, Apr. 2015.

[9] Y. Xu, W. Zhang, and W. Liu, "Distributed dynamic programming-based approach for economic dispatch in smart grids," *IEEE Transactions on Industrial Informatics*, vol. 11, no. 1, pp. 166-175, Feb. 2015.

[10] X. Wang, Y. Liu, J. Zhao *et al*., "A hybrid agent-based model predictive control scheme for smart community energy system with uncertain DGs and loads," *Journal of Modern Power Systems and Clean Energy*, vol. 9, no. 3, pp. 573-584, May 2021.

[11] H. Xing, Y. Mou, M. Fu *et al*., "Distributed bisection method for economic power dispatch in smart grid," *IEEE Transactions on Power Systems*, vol. 30, no. 6, pp. 3024-3035, Nov. 2015.

[12] Z. Zhang and M. Chow, "Convergence analysis of the incremental cost consensus algorithm under different communication network topologies in a smart grid," *IEEE Transactions on Power Systems*, vol. 27, no. 4, pp. 1761-1768, Nov. 2012.

[13] Z. Zhang, X. Ying, and M. Chow, "Decentralizing the economic dispatch problem using a two-level incremental cost consensus algorithm in a smart grid environment," in *Proceedings of 2011 North American Power Symposium*, Boston, USA, Aug. 2011, pp. 1-7.

[14] G. Hug, S. Kar, and C. Wu, "Consensus + innovations approach for distributed multiagent coordination in a microgrid," *IEEE Transactions on Smart Grid*, vol. 6, no. 4, pp. 1893-1903, Jul. 2015.

[15] P. Li, Y. Liu, H. Xin *et al*., "A robust distributed economic dispatch strategy of virtual power plant under cyber-attacks," *IEEE Transactions on Industrial Informatics*, vol. 14, no. 10, pp. 4343-4352, Oct. 2018.

[16] Y. Sun, X. Wu, J. Wang *et al*., "Power compensation of network losses in a microgrid with BESS by distributed consensus algorithm," *IEEE Transactions on Systems, Man, and Cybernetics: Systems*, vol. 51, no. 4, pp. 2091-2100, Apr. 2021.

[17] G. Wen, X. Yu, Z. Liu *et al*., "Adaptive consensus-based robust strategy for economic dispatch of smart grids subject to communication uncertainties," *IEEE Transactions on Industrial Informatics*, vol. 14, no. 6, pp. 2484-2496, Jun. 2018.

[18] Q. Li, D. W. Gao, H. Zhang *et al*., "Consensus-based distributed economic dispatch control method in power systems," *IEEE Transactions on Smart Grid*, vol. 10, no. 1, pp. 941-954, Jan. 2019.

[19] W. Liu, W. Gu, X. Yuan *et al*., "Fully distributed control to coordinate charging efficiencies for energy storage systems," *Journal of Modern Power Systems and Clean Energy*, vol. 6, no. 5, pp. 1015-1024, Sept. 2018.

[20] X. Yu and Y. Xue, "Smart grids: a cyber-physical systems perspective," *Proceedings of the IEEE*, vol. 104, no. 5, pp. 1058-1070, May 2016.

[21] Y. Wang, D. Liu, X. Xu *et al*., "Cyber-physical power system modeling for timing-driven control of active distribution network," *Journal of Modern Power Systems and Clean Energy*, vol. 8, no. 3, pp. 549-556, May 2020.

[22] K. J. Astrom and P. Kumar, "Control: a perspective," *Automatica*, vol. 50, no. 1, pp. 3-43, Jan. 2014.

[23] Z. Zhang and M. Chow, "The influence of time delays on decentralized economic dispatch by using incremental cost consensus algorithm," in *Control and Optimization Methods for Electric Smart Grids*. New York: Springer, 2012, pp. 313-326.

[24] T. Yang, D. Wu, Y. Sun *et al*., "Impacts of time delays on distributed algorithms for economic dispatch," in *Proceedings of 2015 IEEE PES General Meeting*, Denver, USA, Jul. 2015, pp. 26-30.

[25] B. Huang, L. Liu, H. Zhang *et al*., "Distributed optimal economic dispatch for microgrids considering communication delays," *IEEE Transactions on Systems, Man, and Cybernetics: Systems*, vol. 49, no. 8, pp. 1634-1642, Aug. 2019.

[26] J. Yan, J. Cao, and Y. Cao, "Distributed continuous-time algorithm for economic dispatch problem over switching communication topology," *IEEE Transactions on Circuits and Systems II: Express Briefs*, vol. 68, no. 6, pp. 2002-2006, Jun. 2021.

[27] Y. Zhu, W. Yu, and G. Wen, "Distributed consensus strategy for economic power dispatch in a smart grid with communication time delays," in *Proceedings of 2016 IEEE International Conference on Industrial Technology (ICIT)*, Taipei, China, Mar. 2016, pp. 14-17.

[28] G. Chen and Z. Zhao, "Delay effects on consensus-based distributed economic dispatch algorithm in microgrid," *IEEE Transactions on Power Systems*, vol. 33, no. 1, pp. 602-612, Jan. 2018.

[29] U. Munz, A. Papachristodoulou, and F. Allgower, "Delay robustness in non-identical multi-agent systems," *IEEE Transactions on Automatic Control*, vol. 57, no. 6, pp. 1597-1603, Jun. 2012.

[30] Y. Zhang, Y. Sun, X. Wu *et al*., "Economic dispatch in smart grid based on fully distributed consensus algorithm with time delay," in *Proceedings of 2018 37th Chinese Control Conference (CCC)*, Wuhan, China, Jul. 2018, pp. 25-27.

[31] F. Guo, C. Wen, J. Mao *et al*., "Distributed economic dispatch for smart grids with random wind power," *IEEE Transactions on Smart Grid*, vol. 7, no. 3, pp. 1572-1583, May 2016.

[32] F. Guo, C. Wen, J. Mao *et al*., "Distributed cooperative secondary control for voltage unbalance compensation in an islanded microgrid," *IEEE Transactions on Industrial Informatics*, vol. 11, no. 5, pp. 1078-1088, Oct. 2015.

[33] Z. Yang, J. Xiang, and Y. Li, "Distributed consensus based supply de-

mand balance algorithm for economic dispatch problem in a smart grid with switching graph," *IEEE Transactions on Industrial Electronics*, vol. 64, no. 2, pp. 1600-1610, Feb. 2017.
[34] S. S. Reddy, P. R. Bijwe, and A. R. Abhyankar, "Real-time economic dispatch considering renewable power generation variability and uncertainty over scheduling period," *IEEE Systems Journal*, vol. 9, no. 4, pp. 1440-1451, Dec. 2015.
[35] Y. Li, S. Miao, X. Luo *et al*., "Day-ahead and intra-day time scales coordinative dispatch strategy of power system with compressed air energy storage," *Proceedings of the CSEE*, vol. 38, no. 10, pp. 2849-2860, May 2018.

Yuhang Zhang received the B.S. degree from Jiangsu University, Zhenjiang, China, in 2016. He is currently pursuing the Ph.D. degree in electrical engineering in Hohai University, Nanjing, China. His research interests include cyber-physical power system (CPPS), distributed optimization, and cyber security.

Ming Ni received the B.S. and M.S. degrees in electrical engineering from Southeast University, Nanjing, China, in 1991 and 1996, respectively. He is currently the Chief Expert of Power System Analysis and Planning at NARI Technology Co., Ltd., Nanjing, China. He is also an Adjunct Professor with the College of Energy and Electrical Engineering, Hohai University, Nanjing, China. His current research interests include CPPS, stability and control of power systems.

Yonghui Sun received the Ph.D. degree in electrical engineering from the City University of Hong Kong, Hong Kong, China, in 2010. He is currently a Professor with the College of Energy and Electrical Engineering, Hohai University, Nanjing, China. His research interests include CPPS, stability analysis and control of power systems, and optimization algorithms.